Preprint Title	I_2/H_2O_2 mediated synthesis and photophysical properties of imidazole-fused heterocycles via [4+1] cyclization approach
Authors	Haonan Li, Chenping Gao, Qingjie Liu, Yanchun Guo, Shuxia Cao and Yufen Zhao
Publication Date	07 Feb. 2024
Article Type	Full Research Paper
Supporting Information File 1	Supporting Information-BJOC0206.pdf; 14.0 MB
ORCID® iDs	Yanchun Guo - https://orcid.org/0000-0003-1214-5525

I_2/H_2O_2 mediated synthesis and photophysical properties of imidazole-fused heterocycles via [4+1] cyclization approach

Haonan Li[1], Chenping Gao[1], Qingjie Liu[1], Yanchun Guo*[1], Shuxia Cao[1] and Yunfen Zhao[1,2]

Address: [1] College of Chemistry, Zhengzhou University, Zhengzhou, Henan 450001, China [2] Institute of Drug Discovery Technology, Ningbo University, Ningbo, Zhejiang 315211, China

Email: Yanchun Guo – ycguo@zzu.edu.cn

* Corresponding author

Abstract

An efficient I_2 (10 mmol%)/H_2O_2 mediated oxidative formal [4+1] cyclization of 2-pyridinemethylamine or o-phenylenediamine (2-aminobenzenethiol) with benzaldehyde via C-N bond formation has been developed. This strategy offers a straightforward approach to imidazo[1,5-a]pyridine and benzimidazole (benzothiazole) derivatives in 65% to 98% yields. Several heterocyclic products exhibit promising blue luminous performance with satisfactory fluorescence quantum yields of up to 64%, large Stokes shifts, and a longer lifetime (7.35 ns). The band gap energies obtained from DFT are also consistent with the absorption spectra.

Keywords

[4+1] cyclization; I_2/H_2O_2 mediated; Imidazo-fused Heterocycles; Photophysical properties; DFT calculations

Introduction

Both imidazo[1,5-a]pyridine and benzimidazole, which consist of an imidazole moiety fused to a hexacyclic aromatic ring, are important biologically active nitrogen-containing heterocycles. They are well-known for their medicinal use and material applications [1,2]. Imidazo[1,5-a]pyridine and benzimidazole derivatives possess various bioactivities, including antimicrobial, anthelmintic, antiviral, anticancer, and antihypertensive activities. Many compounds possessing imidazo[1,5-a]pyridine or benzimidazole skeleton have been employed as drugs in the market [3,4]. As classic building blocks, imidazo[1,5-a]pyridine and benzimidazole are easily functionalized by introducing substituents in different positions, which leads to a wide range of promising applications in dyes, polymers, metal ligands, organocatalysts, and organic optoelectronic materials [5-12]. For all of these reasons, imidazo[1,5-a]pyridines and benzimidazoles are attracting growing attention among researchers worldwide and engaged in very different research fields.

Although several methods have been explored for efficient synthesis of imidazopyridines and benzimidazoles, most focus on condensation-cyclization methods, including [3+2] / [3+1+1] / [4+1] and by itself [2,13-18]. In comparison, the [4+1] cyclization method, is a more attractive option due to the easy availability of raw materials. In 2009, Shibahara et al. described the synthesis of 1,3-diarylimidazo[1,5-a]pyridines by [4+1] cyclization of aryl- 2-pyridylmethylamines and aldehydes using elemental sulfur as the oxidant [19]. In 2020, Bhalla's group established an efficient

photoredox system for the [4+1] synthesis of benzimidazoles by “Metal-Free” Nano-assemblies of AIEE-ICT-active pyrazine derivatives [20]. Iodine and low concentrations of oxidant hydrogen are widely used in synthesizing heterocyclic compounds because of their potential reactivity and environmental friendliness [21]. Recent examples [22-26] include the iodine-promoted [4+1] synthesis of 1-iodoimidazo[1,5-a]pyridines via sequential dual oxidative C(sp^3)-H amination/C(sp^3)-H iodination reaction of aryl methyl ketones with pyridin-2-ylmethylamines and I_2-mediated intramolecular C-H amidation for the synthesis of N-substituted benzimidazoles [27]. Meanwhile, H_2O_2-mediated [4+1] cycloadditions under metal-free are uncommon. In this regard, only examples of [5+1] cycloadditions have been reported independently, including the synthesis of quinazoline derivatives by Yang et al.[28] and our group [29].

The optoelectronic features of imidazo[1,5-a]pyridines and benzimidazoles are remarkable since the molecules based on them display unique photophysical properties with quantum yields ranging from moderate to high, huge Stokes shift, and good stability under the tested conditions. Specifically, applications of imidazo[1,5-a]pyridines and benzimidazoles in organic optoelectronic materials include organic light-emitting devices (OLEDs) [30,31], nonlinear optic materials (NLOs) [32,33], photosensitizers based on organic metal complexes [34,35], fluorescence cell imaging [36,37], organic fluorescent probes [38-42], sensors and emitters for confocal microscopy [17] and so on. In the design of fluorescent dyes and fluorescent materials, introducing strong electron donors and extending the molecular π-conjugated system has been proven to be an efficient strategy to lengthen emission wavelengths as well as Stokes shifts [43-48] Besides, fluorescent dyes with electron donors can retain a relatively high fluorescent quantum yield, which is determined by the gap between frontier orbitals [49-53].

Given this, it is crucial to develop green and efficient synthetic strategies with a

broad substrate scope to prepare functionalized imidazole-fused heterocycle compounds. At the same time, a systematic study of the photophysical properties of imidazo[1,5-a]pyridine and benzimidazole derivatives is also necessary to understand the relationship between chemical structure and photophysical behavior. Therefore, we report here the synthesis of aryl-substituted imidazo[1,5-a]pyridines and benzimidazoles by I_2/H_2O_2-assisted [4+1] cyclization reaction and evaluation of their photophysical properties. In addition, absorption and emission spectra, quantum yields as well as fluorescence lifetime were measured in solution and interpreted based on density functional theory (DFT) calculations.

Results and Discussion

Synthesis

We started our investigation by studying the reaction of 2-pyridinemethanamine **1a** and benzaldehyde **2a** (Table 1). After numerous trials, when a solution of **1a** (0.8 mmol) and **2a** (0.4 mmol) was treated with I_2 (10 mmol%)/30% H_2O_2 (3 mmol) mediated system in N, N-dimethylformamide at 70 ^oC under an atmosphere of air, [4+1] cyclization product **3a** obtained in 62% in 1.5 h (entry 1). When the same reaction was performed by changing the loading of hydrogen peroxide (entries 2-4) or the material ratios of **1a**:**2a** (I.e, 4:1, 1:1, 2:3, 1:2) (entries 5-8), it was found that some improvement in yield of **3a** was observed. It is worth mentioning that when the amount of **2a** is greater than or equal to **1a**, two products **3a** and **3b** were obtained simultaneously (entries 6-8). Various types of solvents (DMSO, CH_3CN, THF, Dioxane, DCE, H_2O, CH_3CH_2OH) were used under the same reaction condition (entries 9-15), and the best solvent was found to be CH_3CN with 82% yield of **3a** with no traces of compound **3b** (entry 10). Removal of catalyst I_2 resulted in no formation of **3a**, proving the crucial role of I_2 in the

[4+1] cyclization for the C−N bond formation (entry 16c). Other oxidants such as molecular oxygen (O_2) and potassium persulfate ($K_2S_2O_8$) were screened under the same conditions in CH_3CN solvent, but no further improvement in yields was observed (entries 17d and 18e). Further, reaction time (1 h, 3 h, 5 h) and reaction temperature (40 ^oC, 60 ^oC, 80 ^oC) were also screened (entries 19[f]-21[h] and 22[i]-24[k]). Thus, the optimized conditions that produced the best yield of **3a** were 2-pyridinemethanamine (**1a**, 0.8 mmol), benzaldehyde (**2a**, 0.4 mmol), I_2 (10 mmol %), and H_2O_2 (3 mmol) in CH_3CN (5.0 mL) at 60 ^oC for 3 h. Since changing the **1a**:**2a** ratio from 2:1 to 1:2 could lead to different products, we also screened the amount of I_2 and H_2O_2, solvents, reaction temperature, and times to achieve the maximum yield for **3b** (Table S1, in Supporting Information).

Table 1: Optimization of the Reaction Conditions[a].

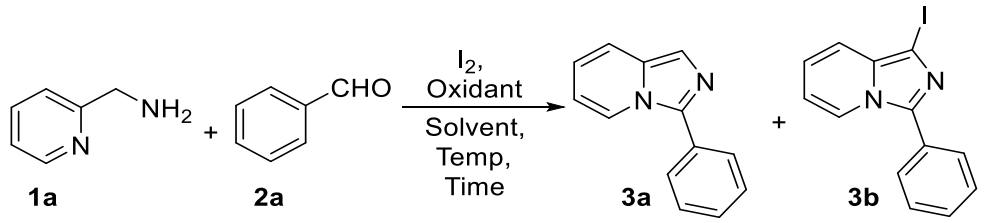

entry	H_2O_2 (mmol)	1a:2a	solvent	Yield[b] (**3a** %)	Yield[b] (**3b** %)
1	0.8	2:1	DMF	62	0
2	1.6	2:1	DMF	73	0
3	3	2:1	DMF	78	0
4	3.5	2:1	DMF	71	0
5	3	4:1	DMF	64	0
6	3	1:1	DMF	44	16
7	3	2:3	DMF	49	22
8	3	1:2	DMF	52	24
9	3	2:1	DMSO	76	0
10	3	2:1	CH_3CN	82	0
11	3	2:1	THF	35	0
12	3	2:1	Dioxane	0	0
13	3	2:1	DCE	42	0
14	3	2:1	H_2O	15	0
15	3	2:1	CH_3CH_2OH	37	0
16[c]	3	2:1	CH_3CN	0	0

17[d]	-	2:1	CH_3CN	53	0
18[e]	-	2:1	CH_3CN	70	0
19[f]	3	2:1	CH_3CN	79	0
20[g]	3	2:1	CH_3CN	83	0
21[h]	3	2:1	CH_3CN	73	0
22[i]	3	2:1	CH_3CN	55	0
23[j]	3	2:1	CH_3CN	84	0
24[k]	3	2:1	CH_3CN	79	0

[a] (Conditions: **1a** (0.8 mmol), **2a** (0.4 mmol), catalyst (10 mmol%), H_2O_2 (3 mmol), solvent (5 mL), 3 h, 60 °C, in an oil bath, Condensing tube, [b]isolated yield. [c]I_2 (0 mmol). [d]O_2. [e]$K_2S_2O_8$ (3 mmol). [f]1 h. [g]3 h. [h]5 h. [i]40 °C. [j]60 °C. [k]80 °C.)

With the optimized conditions in hand, the general substrate scope and tolerability of this [4+1] cyclization protocol were assessed concerning benzaldehyde. The reaction tolerated a wide range of functional groups and various derivatives (**3a-3aac**) were successfully synthesized in 60%-98% yields (Scheme 1). Benzaldehyde with electron-withdrawing groups (-F, -Cl, -Br, $-NO_2$, -CN, $-CF_3$) gave a yield slightly higher than that of electron-donating groups (-Me, -OMe). Further, 2-naphthaldehyde also gave a satisfactory yield (**3au**). Other heterocyclic aldehydes like 2-thiophenecarboxaldehyde, 2-furancarboxaldehyde, 4-thiazolecarboxaldehyde, and 2/3/4-pyridinecarboxaldehyde were well tolerated under these conditions (**3av-3aaa**). 2-pyridinemethanamine bearing fused benzene or pyridine, as di(pyridin-2-yl)methenamine and phenyl(pyridin-2-yl)methanamine delivered **3aab** (69%) and **3aac** (76%), respectively. Moreover, for iodine-substituted 3-phenylimidazo[1,5-a]pyridine derivatives, the corresponding iodination products (**3b-3bba**) were obtained in 70-98% yields as well. However, di(pyridin-2-yl)methanamine and phenyl(pyridin-2-yl)methanamine were less reactive for the iodination of C1-H bonds; therefore, they gave only trace amounts of the products. The results were summarized in Scheme 2. The structures and stereochemistry of the synthesized products were confirmed by the X-ray structures of **3au** (CCDC 2217577) and **3bo** (CCDC 2217551).

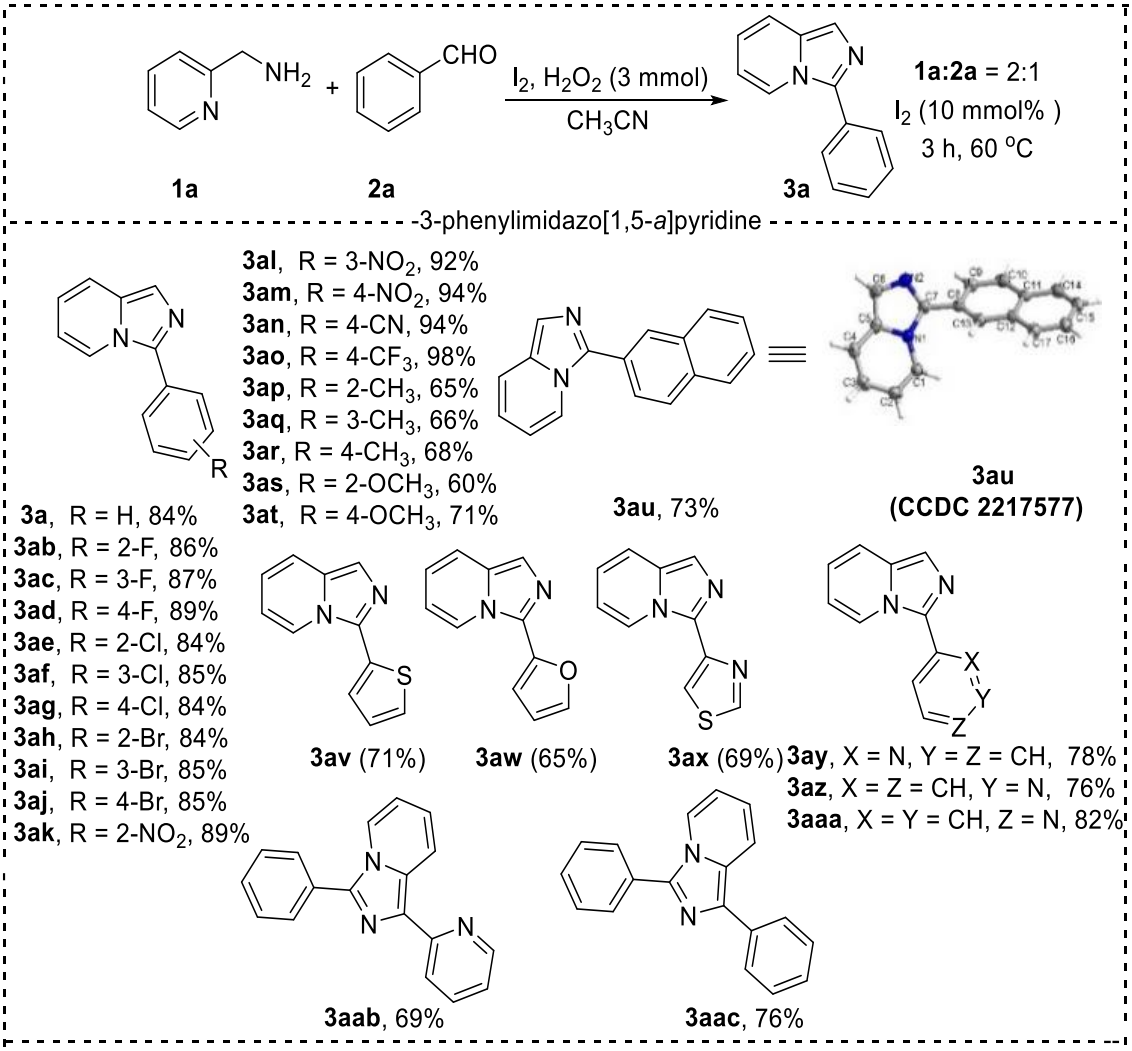

[a]Reaction conditions: **3a: 1a** (0.8 mmol), **2a** (0.4 mmol), I_2 (10 mmol%), 3 h, 60 °C, H_2O_2 (3 mmol), CH_3CN (5 mL), in an oil bath, opened tube, [b]isolated yield.

Scheme 1: Substrate Scope of Imidazo[1,5-a]pyridines

The present [4+1] strategy was also applied for the synthesis of diverse 2-phenyl-1H-benzo[d]imidazoles from benzene-1,2-diamine and benzaldehyde (Scheme 3). Using the optimized reaction condition (details of optimal reaction conditions see Table S2), benzaldehyde with electron-rich or electron-poor substituents in the ortho-, meta- or para-positions (including -Me, -OMe, -F, -Cl, -Br, $-NO_2$, -CN, and $-CF_3$) of benzene all were competent substrates, offering 2-phenyl-1H-benzo[d]imidazoles in 83%-98% yields (**3c−3ct**). N-methyl-substituted benzene-1,2-diamine furnished the desired 1,2-disubstituted benzimidazole **3cu** in 90% yield. When the 2-aminobenzenethiol was employed with 4-methoxybenzaldehyde or 3/4-bromobenzaldehyde, [4+1] cyclization

reaction also could proceed smoothly and offered corresponding product **3cv**, **3cw**, and **3cx** in good yield (68%, 89%, and 91%). Ultimately, the structure of 2-(2-methylphenyl)-1H-benzimidazole and 4-(1H-benzo[d]imidazol-2-yl) benzonitrile was confirmed by single-crystal X-ray structure analysis of **3cb** (CCDC 2235837) and **3cs** (CCDC 2235130).

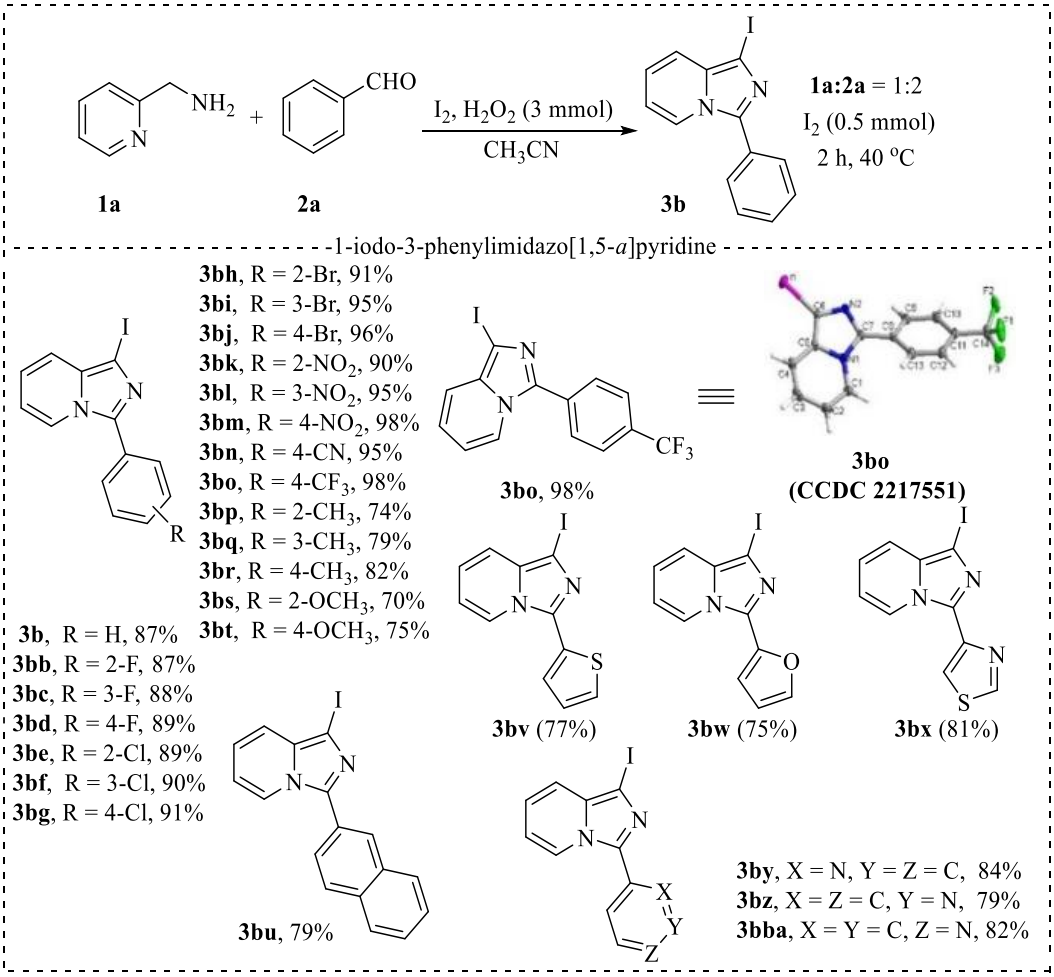

[a]Reaction conditions: **3b: 1a** (0.8 mmol), **2a** (1.6 mmol), I_2 (0.5 mmol), 2 h, 40 °C, H_2O_2 (3 mmol), CH_3CN (5 mL), in an oil bath, opened tube, [b]isolated yield.

Scheme 2: Substrate Scope of 1-iodo-3-phenylimidazo[1,5-a]pyridine

To gain insight into the mechanism of the [4+1] cyclization reaction, the control experiments were performed and shown in Scheme S1. The reaction was not inhibited by the addition of the radical quenchers TEMPO and BHT under standard conditions, suggesting that the reaction may not involve a radical process (Scheme S1a). Without I_2, both products **3a** and **3b** were undetectable (Scheme S1b), indicating that molecular

iodine is essential for the [4+1] cyclization reaction. **3b** was obtained in 69% yield from the reaction of **3a** and I_2/H_2O_2 (Scheme S1c), suggesting that **3a** may be an intermediate product to produce **3b**. When **1a** and **2a** were reacted with equal amounts of CH_3COOH or benzoic acid, the products **3b** were isolated in 92% and 96% yields, respectively, indicating that the protonic acid can effectively promote the reaction to produce **3b** and also explaining the reason for the excess of **2a**. When the reactions were carried out with oxygen, air, and nitrogen instead of H_2O_2, it was found that only a small amount of **3a** and no **3b** was produced in oxygen or air, while both reactions hardly occurred in nitrogen. This suggests that H_2O_2 has a dual role as both a source of oxygen and an initiator of the iodination reaction (Scheme S1d and e).

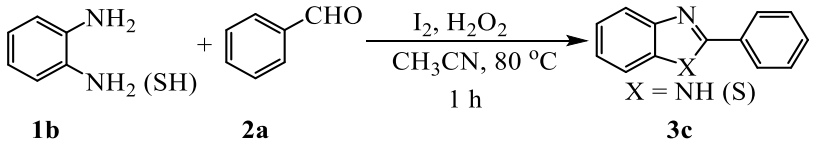

1b **2a** **3c**

3c, R = H, 90%
3cb, R = 2-CH_3, 84%
3cc, R = 3-CH_3, 86%
3cd, R = 4-CH_3, 89%
3ce, R = 2-OCH_3, 83%
3cf, R = 4-OCH_3, 87%
3cg, R = 2-F, 88%
3ch, R = 3-F, 91%
3ci, R = 4-F, 93%
3cj, R = 2-Cl, 90%

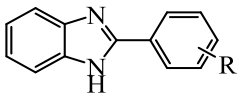

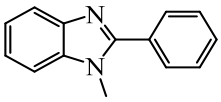

3cu, 90%

3ck, R = 3-Cl, 93%
3cl, R = 4-Cl, 95%
3cm, R = 2-Br, 91%
3cn, R = 3-Br, 92%
3co, R = 4-Br, 96%
3cp, R = 2-NO_2, 87%
3cq, R = 3-NO_2, 89%
3cr, R = 4-NO_2, 91%
3cs, R = 4-CN, 96%
3ct, R = 4-CF_3, 98%

3cb CCDC 2235837

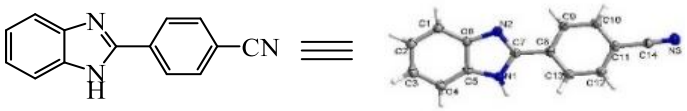

3cs CCDC 2235130

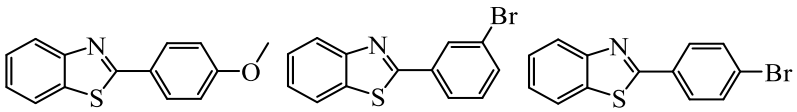

3cv, 68% **3cw**, 89% **3cx**, 91%

[a]Reaction conditions: **1b** (1 mmol), **2a** (1.75 mmol), I_2 (10 mmol%), H_2O_2 (7 mmol), About 1 h, 80 °C, CH_3CN (5 ml), in an oil bath, opened tube, [b]isolated yield.

Scheme 3: Substrate Scope of benzimidazoles

Based on the above results and previous reports [54, 55], a possible mechanism was proposed and outlined in Scheme 4. Initially, HOI was generated from iodine and hydrogen peroxide, and part of the benzaldehyde (**2a**) was oxidized by hydrogen peroxide to benzoic acid. Next, the aldehyde **2a** was attacked by pyridine methylamine (**1a**) to afford the intermediate iminium ion **A** in the presence of molecular iodine, which would be further attacked by the nitrogen of pyridine to give the intermediate **B**. Subsequently, intermediate **B** released H^+ to give intermediate **C**, which was then oxidized to provide the desired product **3a**. In addition, product **3a** could also be iodinated using HOI via an electrophilic attack of I^+ on the C-3 position of **3a** to provide another desired product **3b**.

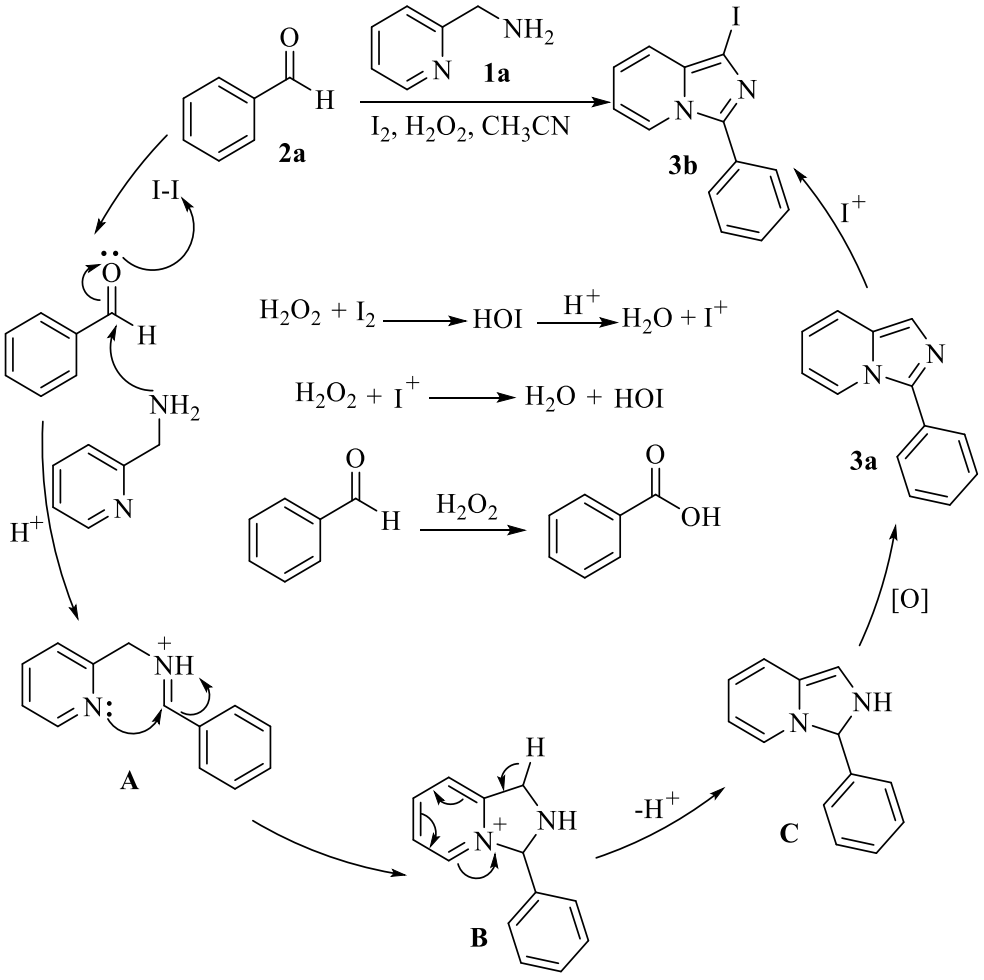

Scheme 4: Possible mechanisms

Photophysical properties and Theoretical calculations

Interestingly, these imidazopyridines and benzimidazoles could be observed to have blue or blue-green fluorescence under illumination with a UV lamp (shown in Figure S1). So the photophysical properties of selected compounds **3a**, **3b**, **3ab**, **3ac**, **3ad**, **3an**, **3ao**, **3ar**, **3at**, **3au**, **3av**, **3aw**, **3ax**, **3ay**, **3az**, **3aaa**, **3aab**, **3aac**, **3c**, and **3cu** were studied and summarized in Table S3, S4, and Figure 1. The absorption and fluorescence spectra of π-extended imidazole-fused aromatic polycycles **3an**, **3aw**, **3ay**, **3aaa**, **3aac**, **3c**, and **3cu** are recorded in different solvents (DMSO, MeOH, Dioxane, and DCM) and shown in Figures 1 and S2, respectively. As displayed in Figures 1a-1g, the absorption bands of these compounds are located in the range of 288-368 nm, while the emission wavelengths lie in the blue region of 428-491 nm, except for **3c** and **3cu** (355-368nm). Functional group modifications on the fused skeleton can affect the self-luminescence properties, electron-donating groups at the benzene of 3-phenyl-imidazo[1,5-a]pyridine moiety lead to a blue shift of absorption wavelength (**3ar**, **3at**) and electron-withdrawing groups lead to a slight redshift of absorption wavelength (**3an** and **3ao**). **3ab**, **3ac**, and **3ad**, due to the different positions of the -F substituents on the benzene ring, the absorption wavelengths of **3ab** and **3ad** have a slight blue shift, and the absorption wavelengths of **3ac** have a slight redshift, which is related to electron-withdrawing inductive effect and electron-donating conjugation of the -F substituent. Increasing the number of conjugated aromatic rings, 3-(naphthal-2-yl)imidazol[1,5-a]pyridine (**3au**), likewise causes a redshift in the absorption wavelength. For the substituents at the C-3 position of the backbone, the heteroaryl group (**3av**, **3aw**, **3ax**, **3ay**, **3az,** and **3aaa**) made the absorption band redshift. When adding I-(**3b**), pyridine-2-yl (**3aab**), and benzene (**3aac**) at C-1 of 3-

phenylimidazo[1,5-a]pyridine moiety compared with **3a**, redshift was also observed at **3b** and **3aab**, but **3aac** has the opposite effect with a significant blueshift in the absorption band. Moreover, the electron-donating methyl employed with the 2-phenyl-1H-benzo[d]imidazole (**3cu**) resulted in the absorption band being blue-shifted compared with **3c**. The $\lambda_{max,\ em}$ values of these substances measured for optical properties have a large stokes shift (4697-12784 cm^{-1}) with a weak dependence on solvent polarity and the quantum yields ranged from 0.04 to 0.64 (Table S4). As displayed in Figure 1 h, emission spectra of selected compounds fit the single exponential function with fluorescence lifetime (τ) varying from 1.76 to 7.35 ns. In addition, photographs of the compounds dispersed in DMSO under visible and UV light are also exhibited (Figure 1i).

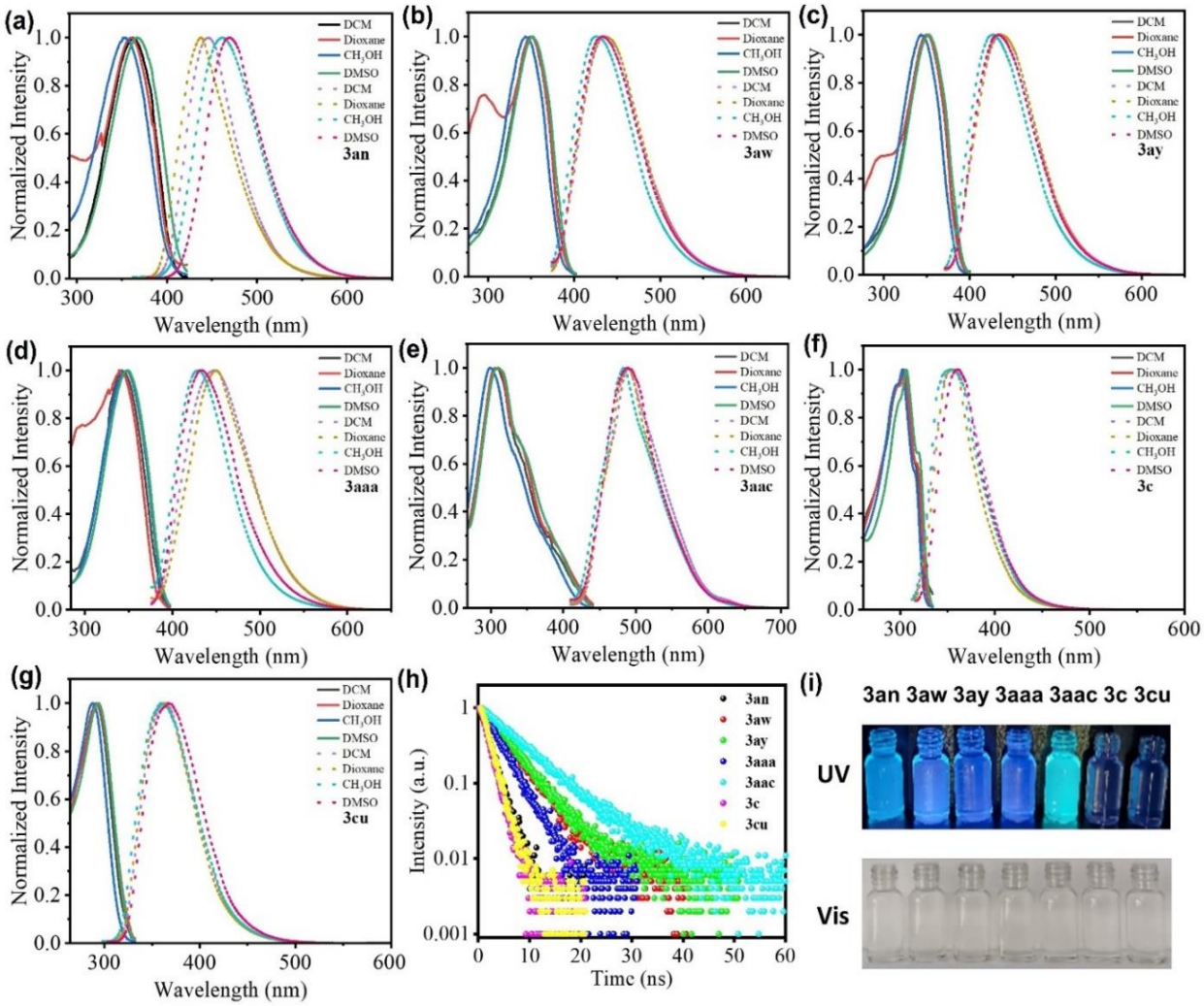

Figure 1： (1a-1g): Absorption (solid lines, 250-450 nm) and emission (dashed lines, 300–700 nm) spectra of the imidazole-fused heterocycles **3an-3cu** in four solvents of different polarity (DCM; Dioxane; CH_3OH; DMSO). The absorption spectra and emission spectra were taken with 1.0×10^{-5} M solutions. (h): Fluorescence lifetime in DMSO. (i): Photos using visible and UV irradiation (λ = 365 nm) in DMSO were taken with 1.0×10^{-4} M solutions.

To better understand the photophysical properties of the selected imidazo[1,5-a]pyridine and benzimidazole compounds, which have larger stokes shifts, time-dependent density functional theory (TDDFT) calculations were performed at the M06-2X/6-31G (d, p) level of theory and equilibrium solutions were also executed. The Frontier Molecular Orbitals of compounds **3an**, **3ay**, and **3aac** are depicted in Figure 3, while similar data for **3a**, **3an**, **3at**, **3ay**, **3aaa**, **3aac**, **3c** and **3cu** can be found in Table S5. TDDFT calculations show that the HOMO and LUMO of each compound are well distributed and the theoretically calculated energy absorption and UV absorption maximum wavelengths are in good agreement with the experimental values. The optimized ground state geometries show that both HOMO and LUMO are delocalized through the imidazopyridine and benzimidazole skeletons (Figure 2 and Table S5). The aryl substituent at the C-3 position also shows electronic contribution, indicating that the presence of the substituted aromatic ring has a significant effect on the photophysical properties of imidazopyridine. The band gap energies (E) of the selected imidazo[1,5-a]pyridine and benzimidazole compounds were obtained from the optimized structures. Comparing compounds **3a** (E = 4.38 eV), **3ay** (E = 3.99 eV), and **3aaa** (E = 4.08 eV), it is evident that incorporating a heteroaromatic ring at the C-3 position significantly narrows the band gap energy of the molecule, consistent with the redshift of UV-vis absorption. Comparing the benzene-substituted compounds, the

substitution of strongly donating (**3at**, R = OMe) and withdrawing (**3an**, R = CN) groups imparted the largest change in the band gap energy at 4.48 eV and 3.80 eV, respectively and UV-vis absorption of **3at** undergoes a significant blueshift, while **3an** undergoes a significant redshift. Adding benzene at C-1 of imidazo[1,5-a]pyridine moiety, as in **3aac** (R_{C-1} = Ph, R_{C-3} = Ph), had a large effect (E = 4.64 eV) in increasing the band gap energy, manifested by a significant blueshift in UV-vis absorption. A comparison of benzimidazole compounds **3c** (E = 4.63 eV) and **3cu** (E = 4.80 eV) indicates that the N-1 substituted methyl group increases the band gap energy, resulting in a blue shift in the UV-vis absorption of **3cu**.

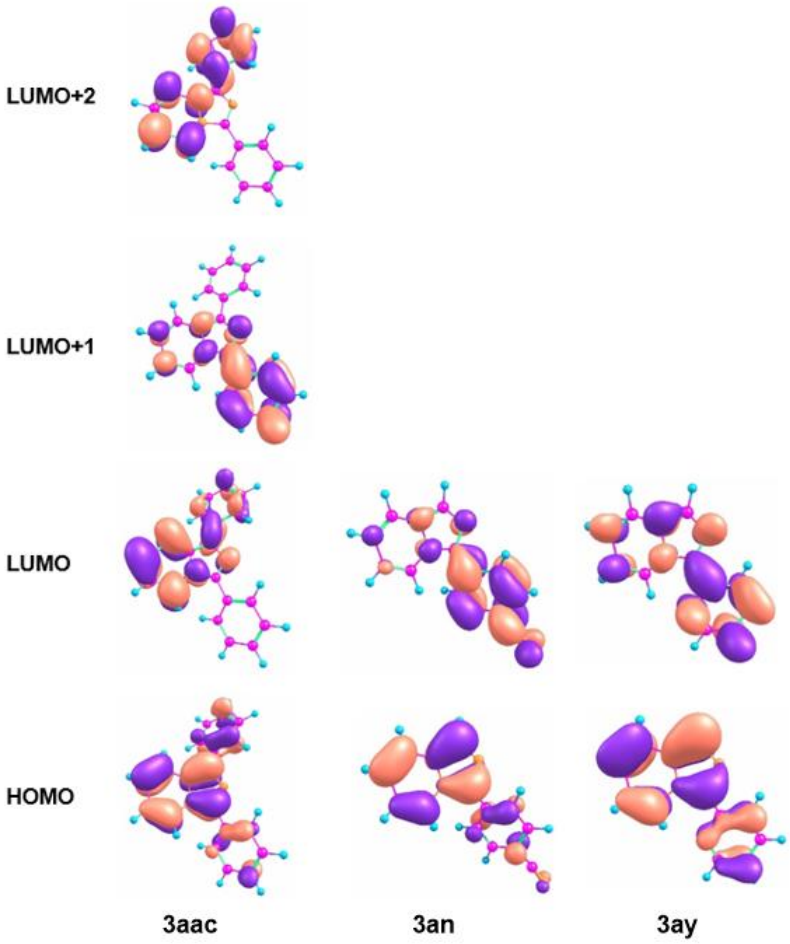

Figure 2： Frontier Molecular Orbitals of compounds **3aac**, **3an** and **3ay**.

Conclusion

In summary, we have successfully developed an efficient I_2/H_2O_2-catalyzed [4 + 1] cyclization method for accessing imidazo[1,5-a]pyridines, 1-iodo-3-phenyl-imidazo[1,5-a] pyridines and 2-phenyl-1H-benzo[d]imidazoles. High synthetic efficiency, mild conditions, simplicity of operation, and a wide range of substrates characterize this method. A plausible mechanism has been proposed in which I_2 is used as the cyclization initiator. Photophysical properties studies have shown that some compounds have large stokes shift, high fluorescence quantum yields, and long lifetimes, suggesting their potential applications in future materials chemistry. The frontier molecular orbitals have been visualized and the HOMO-LUMO energy gap has been calculated. The band gap energies obtained from DFT are also consistent with the absorption spectra.

Experimental

General. Unless otherwise noted, all reactions were carried out under an atmospheric atmosphere. All commercially available chemicals and reagents were used without any further purification unless otherwise indicated. All solvents were dried by standard techniques and distilled before use. Column chromatography was performed on silica gel (200-300 meshes) using petroleum ether (bp. 60~90 °C) and ethyl acetate as eluent. NMR spectra were recorded on a Bruker Avance operating for ^{1}H NMR at 400 MHz, ^{13}C NMR at 101 MHz, and ^{19}F NMR at 376 MHz. NMR spectral data were reported in ppm relative to tetramethylsilane (TMS) as internal standard and $CDCl_3$ (^{1}H NMR δ 7.27, ^{13}C NMR δ 77.0), DMSO (^{1}H NMR δ 5.20, ^{13}C NMR δ 39.52) as solvent. All coupling constants (J) are reported in Hz. The following abbreviations were used to describe peak splitting patterns when appropriate: s = singlet, d = doublet,

dd = double doublet, ddd = double doublet of doublets, t = triplet, dt = double triplet, q = quatriplet, m = multiplet, br = broad. Mass spectra were obtained using Q-Exactive Orbitrap HR-MS (Thermo Fisher Scientific, Waltham, Massachusetts) equipped with an electrospray ion source (ESI) in positive ion acquiring mode. Progress of the reactions was monitored by thin-layer chromatography (TLC). All the amines and aldehydes used here were commercially available. The raw materials used in the reaction were purchased from Aladdin, Macklin, and so on.

UV/Vis spectra were measured by an HP-8453 UV/Vis (Agilent) spectrometer. Fluorescence spectra were tested on the HITACHI F-4600 spectrophotometer which excitation and emission slit width were 5 nm and 10 nm respectively. The fluorescence quantum yield values (Φf) of the compounds in solution were determined by comparing the corrected fluorescence spectra with that of tryptophan in water solution (Φf = 0.13, λexc = 280 nm) as the standard of fluorescence quantum yield [56]. Fluorescence lifetime was determined using the FLS 980 steady-state/transient fluorescence spectrometer instrument. A suitable crystal was selected on an Xcalibur, Eos, and Gemini diffractometer. The crystal was kept at 293 K or 300 K during data collection. Using Olex2 [57], the structure was solved with the Olex2.solve structure solution program using Charge Flipping and refined with the ShelXL[58] refinement pack-age using Least Squares minimization. All of the calculations were carried out using Gaussian 09[59]. The density functional theory (DFT) calculations were performed with the M06-2X functional using the SMD model in DMSO, MeOH, Dioxane, and DCM. Basis set 6-31G(d,p) was employed. Based on the optimized structures at the above level, the TD-DFT calculations were further performed at M06-2X/6-31G (d, p) level with the same solvent effects.

Supporting Information

The Supporting Information is available free of charge on the Beilstein Journal of Organic Chemistry Publications website.

General Experimental Information, Optimization of Reaction Conditions and Control experiment, General Procedure, Photophysical Properties of Selected Products, Experimental Characterization Data for the Products, Copies of NMR Spectra for Compounds (PDF)

Acknowledgements

We thank Dr. Yanyan Wang for the theoretical calculations.

Funding

This work was supported by the National Natural Science Foundation of China (Nos. 21105091).

References

1. Thapa, P.; Palacios, P. M.; Tran, T.; Pierce, B. S.; Foss, Jr. F. W. *J. Org. Chem.,* **2020**, 85, 1991−2009. Doi: 10.1021/acs.joc.9b02714
2. Reddy, M. R.; Darapaneni, C. M.; Patil, R. D.; Kumari, H. *Org. Biomol. Chem.*, **2022**, 20, 3440-3468. Doi: 10.1039/D2OB00386D
3. Lv, S. D.; Han, X. X.; Wang, J. Y.; Zhou, M. Y.; Wu, Y. W.; Ma, L.; Niu, L. W.; Gao, W.; Zhou, J. H.; Hu, W.; Cui, Y. Z.; Chen, J. B. *Angew. Chem., Int. Ed.* **2020**, 59, 11583-11590. Doi: 10.1002/anie.202001510
4. Volpi, G.; Garino, C.; Priola, E.; Magistris, C.; Chierotti, M. R.; Barolo, C. *Dyes Pigm.,*

2019, 171, 107713. Doi: 10.1016/j.dyepig.2019.107713

5. Chen, S.; Li, H. M.; Hou, P. *Anal. Chim. Acta*, **2017**, 993, 63–70. Doi: 10.1016/j.aca.2017.09.016
6. Ge, Y. Q.; Ji, R. X.; Shen, S. L.; Cao, X. Q.; Li, F. Y. *Sens. Actuators B*, **2017**, 245, 875–881. Doi: 10.1016/j.snb.2017.01.169
7. Shen, S.L.; Huang, X.Q.; Lin, X.H.; Cao, X.Q. *Anal. Chim. Acta*, **2019**, 1052, 124-130. Doi: 10.1016/j.aca.2018.11.030
8. Sheng, H. C.; Hu, Y. H.; Zhou, Y.; Fan, S. M.; Cao, Y.; Zhao, X. X.; Yang, W. G. *Dyes Pigm.*, **2019**, 160, 48–57. Doi: 10.1016/j.dyepig.2018.07.036
9. Horton, D. A.; Bourne, G. T.; Smythe, M. L. *Chem. Rev.,* **2003**, 103, 893−930. Doi: 10.1021/cr020033s
10. Harkal, S.; Rataboul, F.; Zapf, A.; Fuhrmann, C.; Riermeier, T.; Monsees, A.; Beller, M. *Adv. Synth. Catal.*, **2004**, 346, 1742−1748. Doi: 10.1002/adsc.200404213
11. Georgiou, I.; Ilyashenko, G.; Whiting, A. *Acc. Chem. Res.*, **2009**, 42, 756−768. Doi: 10.1021/ar800262v
12. Ajani, O. O.; Aderohunmu, D. V.; Ikpo, C. O.; Adedapo, A. E.; Olanrewaju, I. O. *Arch. Pharm.*, **2016**, 349, 475−506. Doi: 10.1002/ardp.201500464
13. Li, M. Y.; Xie, Y.; Ye, Y.; Zou, Y.; Jiang, H. F.; Zeng, W. *Org. Lett.,* **2014**, *16,* 6232-6235. Doi: 10.1021/ol503165b
14. Wang, L. B.; Pan, J.; Tang, C. L.; Bu, X. R.; Wang, J. *Chin. Chem. Lett.,* **2007**, *18*, 390-392. Doi: 10.1016/j.cclet.2007.02.015
15. Pelletier, G.; Charette, A. B. *Org. Lett.,* **2013**, *15*, 2290-2293. Doi: 10.1021/ol400870b
16. Volpi, G.; Rabezzana, R. *New J. Chem.*, **2021**, 45, 5737–5743. Doi: 10.1039/D1NJ00322D
17. Chung, N. T.; Dung, V. C.; Duc, D. X. *RSC Adv.*, **2023**, 13, 32734–32771. Doi:

10.1039/D3RA05960J

18. Faheem, M.; Rathaur, A.; Pandey, A.; Singh, V. K.; Tiwari, A. K. *ChemistrySelect,* **2020**, 5, 3981 –3994. Doi: 10.1002/slct.201904832
19. Shibahara, F.; Sugiura, R.; Yamaguchi, E.; Kitagawa, A.; Murai, T. *J. Org. Chem.,* **2009**, *74*, 3566-3568. Doi: 10.1021/jo900415y
20. Dadwal, S.; Kumar, M.; Bhalla, V. *J. Org. Chem.* **2020**, *85*, 13906-13919. Doi: 10.1021/acs.joc.0c01965
21. Zhu, C. J.; Wei, Y. Y. *ChemSusChem,* **2011**, *4*, 1082-1086. Doi: 10.1002/cssc.201100228
22. Wu, Y. D.; Geng, X.; Gao, Q. H.; Zhang, J. J.; Wu, X.; Wu, A. X. *Org. Chem. Front.,* **2016**, *3*, 1430-1434. Doi: 10.1039/C6QO00313C
23. Wang, Q.; Zha, M.; Zhou, F. L.; Chen, X. X.; Wang, B. Y.; Liu, G. D.; Qian, L. S. *ACS Omega,* **2021**, *6*, 20303-20308. Doi: 10.1021/acsomega.1c02181
24. Bori, J.; Manivannan, V. *J. Heterocycl. Chem.,* **2022**, *59*, 1073-1078. Doi: 10.1002/jhet.4449
25. Hu, J. F.; Li, Y.; Wu, Y. X.; Liu, W.; Wang, Y.; Li, Y. H. *Chem. Lett.,* **2015**, *44*, 645-647. Doi: 10.1246/cl.150133
26. Kulkarni, M. R.; Lad, N. P.; Patil, S. M.; Gaikwad, N. D. *J. Chin. Chem. Soc.,* **2020**, 67, 1887-1894. Doi: 10.1002/jccs.201900516
27. Hu, Z. Y.; Zhao, T.; Wang, M. M.; Wu, J.; Yu, W. Q.; Chang, J. B. *J. Org. Chem.,* **2017**, *82*, 3152-3158. Doi: 10.1021/acs.joc.7b00142
28. Ma, Z. M.; Song, T.; Yuan, Y. Z.; Yang, Y. *Chem. Sci.,* **2019**, *10*, 10283-10289. Doi: 10.1039/c9sc04060a
29. Liu, Q. J.; Chen, H.; Li, S. G.; Guo, Y. C.; Cao, S. X.; Zhao, Y. F. *Chemistryselect,* **2022**, *7*, e202201231. Doi: 10.1002/slct.202201231
30. Mohbiya, D. R.; Sekar, N. *ChemistrySelect,* **2018**, *3*, 1635-1644. Doi:

10.1002/slct.201702579

31. Albrecht, G.; Herr, J. M.; Steinbach, M.; Yanagi, H.; Göttlich, R.; Schlettwein, D. *Dyes Pigm.,* **2018**, *158*, 334-341. Doi: 10.1016/j.dyepig.2018.05.056
32. Fresta, E.; Volpi, G.; Milanesio, M.; Garino, C.; Barolo, C.; Costa, R. D. *Inorg. Chem.,* **2018**, 57, 10469-10479. Doi: 10.1021/acs.inorgchem.8b01914
33. Fresta, E.; Costa, R. D. *J. Mater. Chem. C,* **2017**, *5*, 5643-5675. Doi: 10.1039/C7TC00202E
34. Colombo, G.; Ardizzoia, G. A.; Furrer, J.; Therrien, B.; Brenna, S. *Chem. Eur. J.,* **2021**, *27*, 12380-12387. Doi: 10.1002/chem.202101520
35. Turcio-García, L. Á.; Valdés, H.; Arenaza-Corona, A.; Hernández-Ortega, S.; Morales-Morales, D. *New J. Chem.,* **2023**, *47*, 2090-2095. Doi: 10.1039/D2NJ04699G
36. Volpi, G.; Lace, B.; Garino, C.; Priola, E.; Artuso, E.; Vioglio, P. C.; Barolo, C.; Fin, A.; Genre, A.; Prandi, C. *Dyes Pigm.,* **2018**, *157*, 298-304. Doi: 10.1016/j.dyepig.2018.04.037
37. Saiyasombat, W.; Nuchpun, S.; Katewongsa, K. P.; Pornsuwan, S.; Weigand, J. J.; Kiatisevi, S. *New J. Chem.,* **2022**, *46*, 22525-22532. Doi: 10.1039/D2NJ04508G
38. Ge, Y. Q.; Xing, X. J.; Liu, A. K.; Ji, R. X.; Shen, S. L.; Cao, X. Q. *Dyes Pigm.,* **2017**, 146, 136-142. Doi: 10.1016/j.dyepig.2017.06.067
39. Renno, G.; Cardano, F.; Volpi, G. Barolo, C.; Viscardi, G.; Fin, A. *Molecules,* **2022**, *27*, 3856. Doi: 10.3390/molecules27123856
40. Wu, Y. C.; You, J. Y.; Jiang, K.; Wu, H. Q.; Xiong, J. F.; Wang, Z. Y. *Dyes Pigm.,* **2018**, *149*, 1-7. Doi: 10.1016/j.dyepig.2017.09.043
41. Tang, L. J.; Zhou, L.; Yan, X. M.; Zhong, K. L.; Gao, X.; Liu, X. Y.; Li, J. R. *Dyes Pigm.,* **2020**, *182*, 108644. Doi: 10.1016/j.dyepig.2020.108644
42. Cui, R. L.; Liu, C. H.; Zhang, P.; Qin, K.; Ge, Y. Q. *Molecules,* **2023**, *28*, 515. Doi:

10.3390/molecules28020515

43. Hou, P.; Chen, S.; Wang, H.; Wang, J.; Voitchovsky, K.; Song, X. *Chem. Commun.*, **2014**, 50, 320-322. Doi: 10.1039/C3CC46630B
44. Ren, T. B.; Xu, W.; Zhang, W.; Zhang, X.X.; Wang, Z. Y.; Xiang, Z.; Yuan, L.; Zhang, X. B. *J. Am. Chem. Soc.*, **2018**, 140, 7716-7722. Doi: 10.1021/jacs.8b04404
45. Liu, X. J.; Li, Y.; Ren, X. J.; Yang, Q. W.; Su, Y. A.; He, L.; Song, X. Z. *Chem. Commun.*, **2018**, 54, 1509-1512. Doi: 10.1039/C7CC08154E
46. Geng, Y.; Tian, H. H.; Yang, L.; Liu, X. J.; Song, X. Z. *Sens. Actuators B Chem.*, **2018**, 273, 1670-1675. Doi: 10.1016/j.snb.2018.07.088
47. Liu, X. G.; Cole, J. M.; Xu, Z.C. *J. Phys. Chem. C*, **2017**, 121, 13274-13279. Doi: 10.1021/acs.jpcc.7b04176
48. Cai, Z. B.; Chen, L. J.; Li, S. L.; Ye, Q.; Tian, Y. P. *Dyes Pigm.,* **2020**, 175, 108115. Doi: 10.1016/j.dyepig.2019.108115
49. Chen, W.; Xu, S.; Day, J. J.; Wang, D. F.; Xian, M. *Angew. Chem. Int. Ed.,* **2017**, 56, 16611-16615. Doi: 10.1002/anie.201710688
50. Grabowski, Z. R.; Rotkiewicz, K.; Rettig, W. *Chem. Rev.*, **2003**, 103, 3899-4032. Doi: 10.1021/cr940745l
51. Liu, X.; Qiao, Q.; Tian, W.; Liu, W.; Chen, J.; Lang, M. J.; Xu, Z. C. *J. Am. Chem. Soc.*, **2016**, 138, 6960-6963. Doi: 10.1021/jacs.6b03924
52. Ren, X. J.; Guo, M.; Gong, J. Y.; Zhang, Y.; Yang, L.; Liu, X. J.; Song, X. Z. *Dyes Pigm.,* **2020**, 173, 108007. Doi: 10.1016/j.dyepig.2019.108007
53. Albrecht, G.; Rössiger, C.; Herr, J. M.; Locke, H.; Yanagi, H.; Göttlich, R.; Schlettwein, D. *Phys. status solidi B,* **2020**, *257*, 1900677. Doi: 10.1002/pssb.201900677
54. Wu, Y.; Geng, X.; Gao, Q.; Zhang, J.; Wu, X.; Wu, A. *Org. Chem. Front.* **2016**, *3*, 1430-1434. Doi: 10.1039/C6QO00313C

55. Mahajan, S.; Sawant, S. D. *J. Org. Chem.* **2022**, *87*, 11387-11398. Doi: 10.1021/acs.joc.2c00890

56. Chen, R. F. *Anal. Lett.,* **2006**, *1*, 35-42. Doi: 10.1080/00032710500423377

57. Dolomanov, O. V.; Bourhis, L. J.; Gildea, R. J.; Howard, J. A. K.; Pusch-mann, H. *J. Appl. Crystallogr.* **2009**, *42*, 339-341. Doi: 10.1107/S0021889808042726

58. Sheldrick, G. M. *Acta Crystallogr. Sect. C: Struct. Chem.* **2015**, *71*, 3–8. Doi: 10.1107/S2053229614024218

59. Frisch, M. J.; Trucks, G. W.; Schlegel, H. B.; Scuseria, G. E.; Robb, M. A.; Cheeseman, J. R. Gaussian 09, revision B.01. Gaussian, Inc. Wallingford C T; **2010**.